

Focal Sclerosis of Semicircular Canals With Severe DFNA9 Hearing Impairment Caused by a P51S COCH-Mutation: Is There a Link?

*Sebastien Pierre Janssens de Varebeke, †Bruno Termote, ‡Guy Van Camp,
§Paul J. Govaerts, †Steven Schepers, *Tony Cox, *Kristof Deben,
*Katrien Ketelslagers, and †Geert Souverijns

*Department of Otorhinolaryngology, Campus Virga Jesse, †Department of Radiology, Jessa Hospital, Hasselt; ‡Department of Biomedical Sciences, Medical Genetics Centre, University of Antwerp, Antwerp; and §The Eargroup, Antwerp-Deurne, Belgium

Hypothesis: Focal sclerosis of one or more semicircular canals on computed tomographic (CT) scans and a corresponding signal loss on magnetic resonance (MR) imaging are radiologic lesions that are linked to patients who are suffering from advanced otovestibular impairment caused by hereditary DFNA9 hearing loss.

Background: DFNA9 is a hereditary hearing loss that is characterized by late-onset progressive imbalance and hearing deterioration, caused by mutations in the COCH gene. To date, no radiologic lesions have been associated with this condition.

Study Design: A retrospective chart review

Setting: Tertiary referral center

Subjects: The radiologic data of 9 patients who presented between 2007 and 2012 with otovestibular deterioration caused by a mutation in the COCH gene were reviewed.

Results: All 9 subjects were carriers of the same c.151C > T, p.Pro51Ser (P51S) - missense mutation in the COCH gene. In 8 of them similar sclerotic lesions and/or narrowing were demonstrated in one or more semicircular canals on computed tomography CT scan, with a signal loss at corresponding areas on T2-weighted magnetic resonance (MR) images. In 1 patient,

the posterior part of the vestibule was also affected. The posterior canals were affected in most cases (58%), compared with the superior (21%) and lateral canals (16%) or the vestibule (5%). Only 68.4% of the lesions on MR images were also visible on CT scans, suggesting a fibrotic process without calcification. Ears presenting radiologic lesions showed significantly more severe hearing loss (median PTA 104 dB HL) compared with unaffected ears (58 dB HL).

Conclusion: Eight of 9 subjects with the same P51S mutation in the COCH gene showed similar radiologic lesions, affecting the PSCC in the majority of the cases. These radiologic abnormalities occurred in more advanced stages of the otovestibular deterioration, supporting the hypothesis that these lesions might represent the end phase of a low-grade chronic inflammation or protein deposition. A new phenotypic and characteristic radiologic feature of DFNA9 has been discovered. **Key Words:** COCH mutation—Computed tomography—DFNA9—Hearing loss—Magnetic resonance—Sclerosis—Semicircular canals.

Otol Neurotol 35:1077–1086, 2014.

DFNA9 is an autosomal dominantly inherited nonsyndromic form of hearing loss, caused by mutations in the coagulation factor C homology (COCH)-gene (1996) (1,2). It is characterized by a gradual vestibular deterioration associated with a progressive sensorineural hearing loss, which typically begins in the fourth decade. The hearing impairment starts with a high-frequency loss that declines to very poor auditory performance in the 6th or 7th decade (1–9). Besides DFNA11, it is the only autosomal dominant

hearing loss that is associated with vestibular dysfunction (6). Because a number of DFNA9 carriers exhibit fluctuating hearing loss accompanied with intermittent vertigo and dizziness, aural fullness and tinnitus, this disease may sometimes be misdiagnosed as Ménière's disease or dehiscence superior semicircular canal syndrome (5,10,11). The first vestibular signs usually occur well before the emergence of the hearing loss. The imbalance declines to complete bilateral vestibular areflexia, causing unsteadiness in the dark and head movement-dependent oscillopsia (HMDO) (9).

Many different missense mutations have been identified in the COCH-gene worldwide, of which, the c.151C > T, p.Pro51Ser (P51S), V66G, G88E, I109N, and W117R are the most common mutations. These were found in

Address correspondence and reprint requests to Sebastien Pierre Janssens de Varebeke, M.D., Department of Otorhinolaryngology, Campus Virga Jesse, Jessa Hospital, Stadsomvaart 11, 3500 Hasselt, Belgium; E-mail: drsjanssens@gmail.com

The authors disclose no conflicts of interest.

families from the United States, Australia, Belgium, and The Netherlands (12–15). The majority of these mutations is rare and mostly affect only one family. In contrast, the P51S mutation is a frequent mutation in the low countries (Belgium and The Netherlands), affecting hundreds of patients, clustering in different families (1,6,8). Haplotype analysis has given evidence for a common founder for the Belgian and Dutch families (8).

Histopathologic studies on subjects with hereditary DFNA9 deafness revealed typical accumulation of large amounts of eosinophilic acellular glycosaminoglycan deposits containing cochlin, with a severe atrophy of fibrocytes at the same areas, mainly in the spiral ligament and spiral limbus in the cochlea and in the area of stromal fibrocytes in the crista ampullaris of the semi-circular canal and maculae of the vestibular system. The progressive loss of fibrocytes may be the result of cytotoxicity because of the accumulation of this acellular substance that probably consists of misfolded COCH protein (15–18).

The phenotype of this P51S-mutation has been well documented in several publications, describing typical audiologic and vestibular aspects with very little variability in its expression (2–11).

Hildebrand et al. (11) reported 1 case of a patient with a COCH mutation presenting with bilateral superior semicircular canal (SSCC) dehiscence on computed tomography (CT) imaging. Besides this lesion, although not specifically linked to DFNA9, no other radiologic abnormalities have been described in DFNA9 hearing impaired patients (2–7,9).

In this study, we report a case series in which 8 of 9 patients presented similar focal sclerosis or narrowing of one or more SCC on CT scans and a signal loss on MR imaging in the corresponding areas. All of them were carriers of the same P51S mutation in the COCH gene.

MATERIALS AND METHODS

A retrospective analysis was conducted at our Department of Otorhinolaryngology when we noticed similar radiologic lesions in one or more semicircular canals (SCC) in several patients with COCH otovestibular impairment. Using patient charts, we retrieved all such patients that were seen between 2007 and 2012. Nine patient charts were identified with a documented P51S COCH mutation. For all the selected subjects both CT and MR imaging were available, so all selected subjects could be enrolled in this study. The study was approved by the local medical ethics committee.

MR imaging was performed on 3 machines: A 1.0T system (NT SCAN, Philips, Best, The Netherlands), a 1.5T system (Achieva, Philips, Best, The Netherlands), or a 3T system (Magnetom Skyra, Siemens, Erlangen, Germany). The high-resolution heavily T2-weighted images from the Philips scanner were acquired using a Driven equilibrium (DRIVE) sequence (3D turbo spin echo technique (TSE), echo time (TE) 250 ms, repetition time (TR) 1500 ms; thickness 1.6 mm; spacing 0.8 mm). The Siemens scanner uses an isotropic 3D TSE technique with a restore pulse (TE 317 ms, TR 1400 ms, thickness 0.45 mm, spacing 0 mm).

CT images were acquired using an Aquilion 64 slice scanner (Toshiba Medical Systems, Tokyo, Japan) with the following parameters: kV 120, mA 180, sharp U-HRES filter, thickness 0.5 mm, interval 0.3, scan range 240 mm, field of view (FOV)

114 mm, pitch 5. The spiral CT data volume was reconstructed in an axial plane (thickness 0.6 mm, spacing 0.4 mm; window width 4000, length 800) parallel to the LSCC as well as in a coronal plane perpendicular to the axial plane. This is performed for the temporal bone on both sides.

Cone beam CT (CBCT) images were obtained using a Newtom 5G scanner (QR systems, Verona, Italy) and using the following parameters: FOV 15 × 5 cm, kV 110, mA 20, kernel “standard,” window center 525 and width 3050. CBCT data were subsequently reconstructed with 0.25 mm thickness and 0 mm spacing in a similar orientation as the CT scan.

The images of Patient 9 were acquired in another hospital in 2006. The CT imaging was obtained with a Lightspeed 16 slice scanner (General Electric (GE), Milwaukee, USA) and following parameters: kV 140 and mA 240, FOV (field of view) 25 cm × 0.625 mm, Bone Plus Kernel, window center 500 and width 3000. Axial reconstruction was acquired in FOV 9.6 cm with 0.625 mm thickness and 0.2 mm interval (overlap); coronal reconstructions were obtained with 0.5 mm thickness and 0 mm spacing.

The MR imaging was acquired with a 1.5 T Avanto system (Siemens, Erlangen, Germany) using 3 sequences: a TSE T2-weighted sequence (TE 103, TR 4710, thickness 5 mm, spacing 0.65 mm, number of averages 2), the heavily weighted T2 sequence (3D TSE T2) (TE 303, TR 1500, thickness 0.4 mm, spacing 0 mm), and the T1-weighted sequence (3D gradient echo (GRE) T1 weighted sequence (volumetric interpolated breath-hold (VIBE) sequence) (TE 3.97, TR 1850, thickness 0.7 mm, inversion time 1100, number of averages 1). Reconstructions were obtained for axial and coronal axis in FOV of 17 cm, thickness 1 mm. The antenna was an 8-channel head coil, no surface coils were used at the time the examination was performed (2006). All images were retrospectively reviewed by a dedicated head and neck radiologist.

Audiometry

All pure tone thresholds were measured according to the guidelines of the Committee on Hearing and Equilibrium (19). The pure tone averages (PTA) were calculated for the frequencies 500, 1,000, 2,000, and 3,000 Herz (Hz). All measurements were performed on a calibrated Affinity 2.0 audiometer (Interacoustics, Assens, Denmark).

Vestibular Examination

Three of the 9 affected patients underwent vestibular examination, including saccades, smooth pursuit, and horizontal optokinetic nystagmus responses as well as rotatory chair and bithermal (30°C and 44°C) caloric stimulation in complete darkness. The caloric testing was carried out using binaural alternating caloric stimulation after oculomotor ENG (Fitzgerald-Hallpike method), and asymmetry was calculated on peak slow-phase velocities using the Jongkee’s formula (Aquistar, Nysstar and Ideas I, Difra, Belgium).

RESULTS

Table 1 gives an overview of the 9 patients who are described more in detail in this section. The following data were summarized: pure tone averages (PTA) in decibel hearing level (dBHL), age of subject at time of CT scan and/or MRI (in yr) as well as the presence of vestibular symptoms, results of documented vestibular electronystagmography (ENG), if available, and the description of the radiologic findings. The vestibular signs are further described in detail in Table 2, with special interest to age of

TABLE 1. Overview of the patient’s data: age (years), hearing thresholds (PTA), vestibular symptoms/anomalies, and lesions on computed tomographic scan and MRI of the patient series

Patient	Sex (F/M)	Age	PTA right ear*	PTA left ear*	Vestibular symptoms	Abnormal ENG	CT lesion right ear	CT lesion left ear	MRI signal loss right ear	MRI signal loss left ear
1	M	56	104	76	+	N/A	PSCC (focal)	–	PSCC	–
2	M	65	88	78	+	N/A	SSCC ++	SSCC+	PSCC/SSCC	PSCC/SSCC
3(I)	F	63	83	113	+	N/A	PSCC (narrowing + hyperdensity)	LSCC/SSCC (focal)	PSCC	LSCC/SSCC/PSCC
4(I)	M	61	109	105	+	N/A	PSCC (focal)	PSCC	PSCC	PSCC
5(I)	M	66	104	106	+	N/A	PSCC (total)	PSCC (partial)	PSCC (total)	PSCC (partial)
6(II)	M	65	120	71	+	100% R	PSCC (narrowing)	–	PSCC (subtotal)/SSCC	–
7(II)	F	49	36	40	+	41% R	–	–	–	–
8****(III)	M	46	62	8	+	N/A	–	–	–	–
		51	90	58	+	100% R	PSCC (hyperdensity)	–	PSCC (LSCC)	–
9(III)	F	80	100	95	+	N/A	–	LSCC	Vestibule	LSCC

*PTA (pure tone averages calculated for the frequencies 500, 1,000, 2,000, and 3,000 Hz).

I: family I: Patients 3, 4, and 5 are siblings (brothers/sister).

II: family II: Patients 6 and 7 are siblings (brother/sister).

III: family III: Patients 8 and 9 are siblings (mother/son).

**** for patient 8, both PTA at the 2 visits with 5-year interval are included; SCC indicates semicircular canal; P, posterior; L, lateral; S, superior; and N/A, nonavailable.

emergence of the vestibular signs and details of vestibulo-ocular reflex (VOR) tests, when available.

Many of the selected patients were relatives, and 3 different families were identified. For the sake of clarity, in Tables 1 and 2, all members of the same family were assigned the

Roman numerals ‘‘I, II, and III’’ next to their corresponding patient number.

All the selected patients were Caucasian, and for all of them, genetic testing revealed the presence of the P51S mutation in the COCH gene. All patients were seen between

TABLE 2. This table shows a more detailed overview of the vestibular signs and function in relationship with the age of the patients, hearing thresholds (dB HL), and radiologic findings

Patient no.	Age (yr) at examination	Age (yr) at first vestibular symptoms	Vestibular symptoms*	Vestibular function (VOR)**	Vestibular signs prominent (Y/N)***	PTA Right (dB HL)\$	PTA Left (dB HL)\$	Radiologic lesion (Y/N)£
1	56	35	Ménière-like, aural fullness, dizziness	N/A	N	104	76	Y(Right ear)
2	65	34	Dizziness, vertigo, HMDO, instability in the dark	N/A	N	88	78	Y(bilateral)
3(I)	63	40	Dizziness, HMDO, instability in the dark	N/A	N	83	113	Y(bilateral)
4(I)	61	35–40#	Dizziness, instability in the dark, HMDO	N/A	N	109	105	Y(bilateral)
5(I)	66	35–40#	Dizziness, instability in the dark, HMDO	N/A	N	104	106	Y(bilateral)
6(II)!	65	33	Ménière-like, aural fullness, dizziness, vertigo	Areflexia at right ear	N	120!	71	Y(right ear)
7(II)	49	31	Dizziness, instability	Severe hyporeflexia (41%) right side	Y	36	40	N
8(III)	46	34	Dizziness	N/A	N	62	8	N
	51	50	Instability in the dark, dizziness, Ménière-like	Areflexia right side	Y	90	58	Y(right ear)
9(III)	80	4th decade#	Dizziness, HMDO, instability in the dark	N/A	N	100	95	Y(bilateral)

*HMDO = head movement-dependent oscillopsia.

**VOR = vestibulo-ocular reflex test (details in method section).

Y/N: Yes/No.

N/A: non available.

***Vestibular signs were quoted as a ‘‘yes’’ whenever the subjects presented with vestibular signs as a predominant complaint.

\$: PTA (dB HL): pure tone averages calculated for the frequencies 500, 1,000, 2,000, and 3,000 Hz.

£: Table 1 for details.

#: indicates whenever a precise age of the onset of the symptoms could not clearly be determined.

!: Patient 6 has previously undergone a surgical intervention to the right ear.

I: family I: Patients 3, 4, and 5 are siblings.

II: family II: Patients 6 and 7 are siblings.

III: family III: patient 8 (son) and 9 (mother).

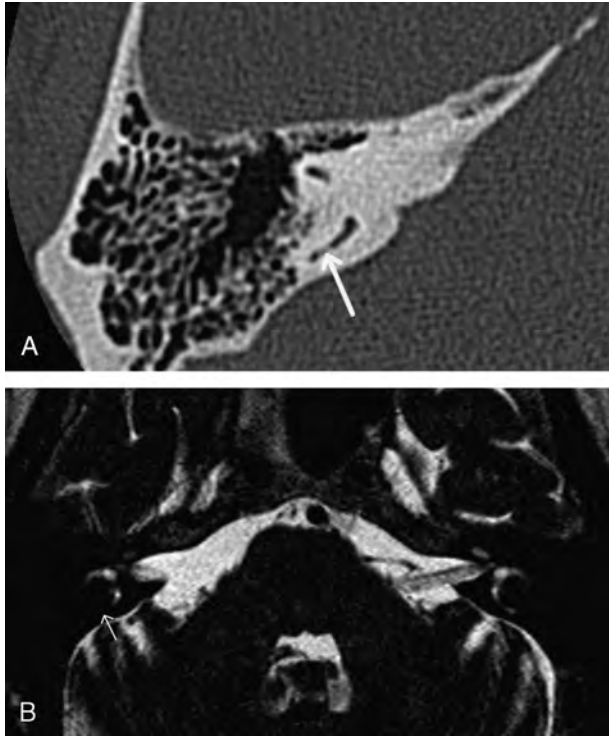


FIG. 1. A and B, CT and MR imaging of Patient 1: (A) patient 1: axial CT scan image of the right temporal bone showing a focal area of sclerosis in the PSCC (arrow). B, Patient 1: axial MR (NT scan) image: absence of fluid signal in the PSCC on the right (arrow) as compared with the left side.

the fifth and eighth decade, ranging from 46 to 80 years (median, 63 yr). Three of 9 subjects were female patients (Table 1). Typically, all patients experienced progressive imbalance and dizziness which began during the third to fourth decade, with increasing unsteadiness in the dark and HMDO developing within the following 10 to 15 years (see Table 2 for details). The vestibular signs were almost never predominant and were only mentioned during targeted history taking in the majority of the cases. Three of 9 patients exhibited more Ménière-like symptoms (Patients 1, 6, and 8; Tables 1 and 2). The vestibular signs were present in all subjects well before the emergence of the hearing loss. All these descriptions are in line with the previously described phenotype of DFNA9 (2–11).

Patient 1 presented to us at the age of 56 years, with complaints of sudden sensorineural hearing loss in the right ear. He had experienced fluctuating imbalance since the age of 35, with a subtle onset and slow progression toward a more Ménière-like syndrome, including aural fullness (Table 2). Pure tone audiometry showed thresholds (average at 500, 1,000, 2,000, 3,000 Hz) of 104 dB HL PTA at the right ear and 76 dB HL PTA at the left ear (Figs. 9, 10 and 11). CT scan images (Fig. 1A) showed a focal area of sclerosis in the posterior semicircular canal (PSCC) on the right side correlating with signal loss in the PSCC at the same site on the heavily T2-weighted

MR images (Fig. 1B) as compared with the normal signal on the patient's left side.

Patient 2, aged 65, presented with severe communication problems even with conventional hearing aids. The hearing thresholds at first presentation were 88 dB HL PTA (right) and 78 dB HL PTA (left) (Figs. 9, 10 and 11). Focal sclerosis of the superior semicircular canal (SSCC) was visible on CT imaging on both sides, although more pronounced on the right side (Fig. 2A). MRI demonstrated focal loss of signal in the left and right SSCC and PSCC on T2-weighted images (Fig. 2B). Figure 2B shows the absence of signal in the anterior limb of the SSCC on the right side corresponding with the findings on CT imaging. However, the T2 hyperintense (fluid) signal on MR imaging was absent in both limbs of the SSCC bilaterally on the more cranial images.

Patient 3 (family I) is the sister of patients 4 and 5 in this study. The hearing levels were 83 dB HL PTA (right) and 113 dB HL PTA (left) (Figs. 9, 10 and 11). Focal sclerosis was demonstrated on CT scans, at the level of the lateral SCC (LSCC) (Fig. 3A) and the anterolateral part of the SSCC of the left ear and a narrowing as well as densification of the PSCC was seen on the right ear, all of which correlated with T2 signal loss on MR imaging (left more than right). The normal fluid signal in the

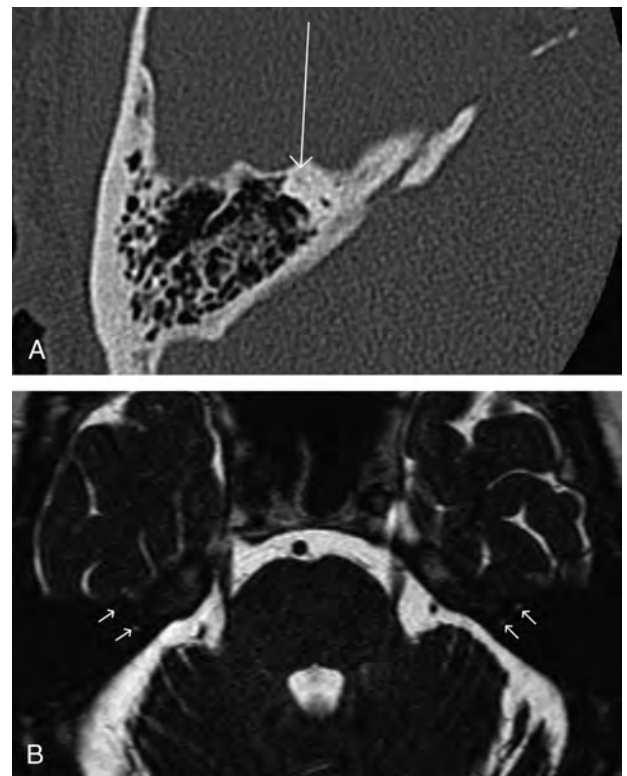


FIG. 2. A and B, CT and MR imaging of Patient 2: (A) Patient 2: axial CT image of the right temporal bone: sclerosis of the anterior part of the SSCC (arrow) as compared with the normal situation in the posterior part. B, patient 2: axial MR (Achieva) image: loss of signal in the anterior part of the SSCC on the (patient's) right as compared with the normal situation in the posterior part and the contralateral side.

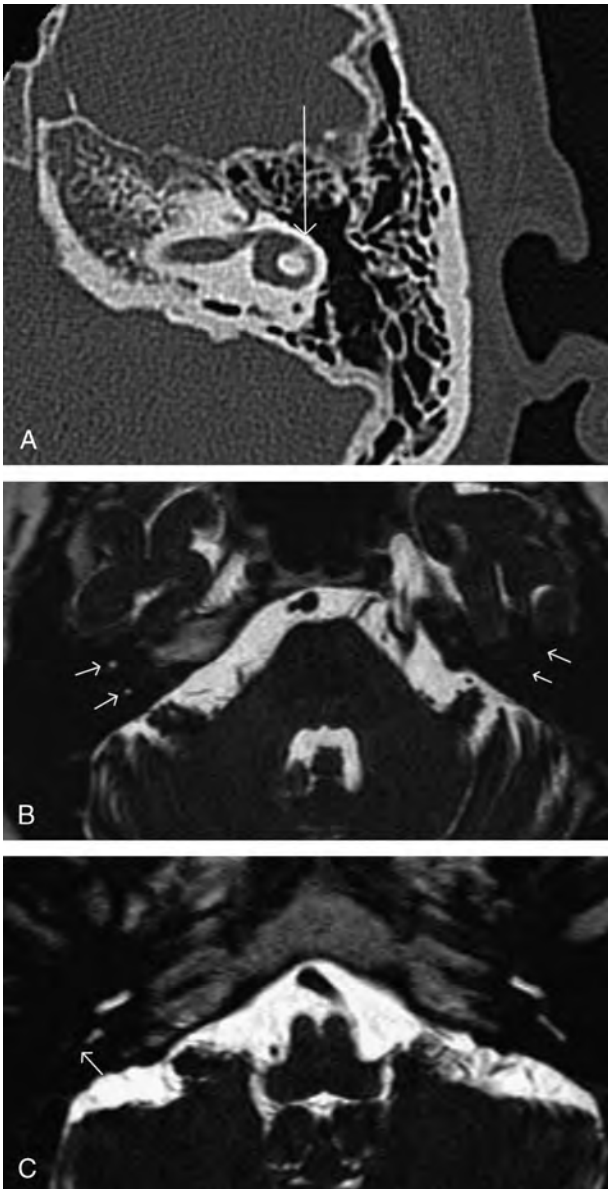


FIG. 3. A, B, and C, CT and MR imaging of Patient 3: (A) Patient 3: axial CT image of the left temporal bone: focal sclerosis of the anterior part of the LSCC (arrow). B, Patient 3: axial MR (Achieva): normal fluid signal in the anterior and posterior limb of the SCC in the right temporal bone; complete signal loss on the patient's left side. C, Patient 3: axial MR (Achieva) image: note the focal signal loss in the posterior part of the right PSCC (arrow) as compared with the normal left side.

SSCC was absent on the patient's left side (Fig. 3B). Note the partial lack of signal in the right PSCC (Fig. 3C).

Patient 4's hearing thresholds were 109 dB HL PTA (right) and 105 dB HL PTA (left) (Figs. 9, 10 and 11). Cone beam computed tomography (CBCT) images (Fig. 4A and B) revealed focal sclerosis of the central third part of the PSCC at both sides, with once more T2 signal loss at the same level on both sides on MR imaging. Note the

partial volume effect in the LSCC bilaterally and the conflicting motion artefacts on the CBCT image warranting correlation with MRI.

The brother of patients 3 and 4, in this study patient 5, was first seen at the age of 66 with hearing loss of 104 dB HL PTA (right) and 106 dB HL PTA (left) (Figs. 9, 10 and 11). Computed tomography (CT) scans showed a total sclerosis of the PSCC on the right and partial sclerosis of the left ear (Fig. 5A). MR images revealed bilateral signal loss in the PSCC (Fig. 5B).

Patient 6 (family II) presented with hearing thresholds of 71 dB HL PTA (left) and 120 dB HL PTA (right) (Figs. 9, 10 and 11). The total deafness at the right side resulted from a previous stapedotomy (10 yr earlier and performed by another surgeon). Besides heavy vertigo and dizziness immediately after surgery, he experienced Ménière-like symptoms. Vestibular ocular reflex-tests (VOR) using electronystagmography (ENG) showed a total areflexia of the right vestibular organ, with directional preponderance to the right on the rotatory chair stimulation tests (21%), although the vestibular signs were not predominant (Table 2). There were no demineralization foci depicting possible otospongiotic foci, neither were there any signs of posterior semicircular canal dehiscence nor large vestibular aqueducts (LVA) on CT imaging. Instead, a narrowing of the right posterior semicircular canal (PSCC) could be seen on these

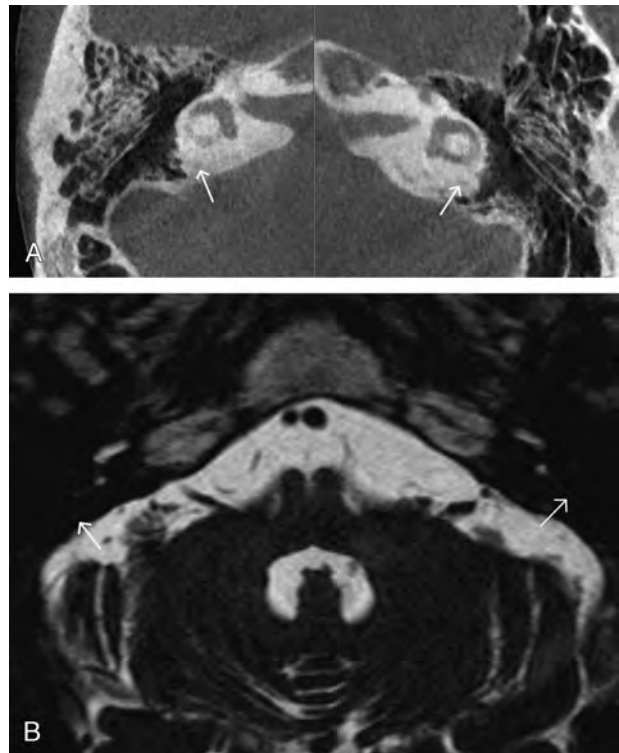


FIG. 4. A and B, CT and MR imaging of Patient 4: (A) Patient 4: axial CBCT image, slightly degraded because of motion artifacts. Bilateral sclerosis of the PSCC (arrows). Partial volume effect in the LSCC on both sides. B, Patient 4: axial MR (Achieva) image showing signal loss in the PSCC bilaterally (arrows).

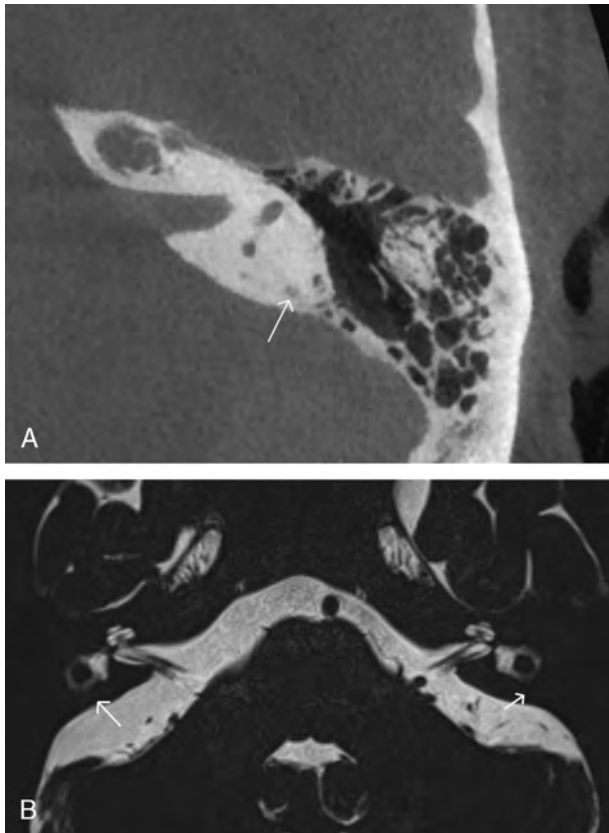


FIG. 5. A and B, CT and MR imaging of Patient 5: (A) Patient 5: axial CT image of the left temporal bone: subtle sclerosis of the PSCC (arrow). Compared with the normal signal in both limbs of the SSCC. B, Patient 5: axial MR (Skyra) image: bilateral absence of signal in the PSCC (arrows).

CT images (Fig. 6A). On MR T2-weighted images signal loss was found in the posterior part of the right SSCC, as well as subtotal obliteration of the PSCC at the same side (Fig. 6B).

The 46-year-old younger sister of the previous patient, in this study, Patient 7, was referred to us with increasing dizziness and tinnitus with hyperacusis since the age of 31. The vestibular signs were described as a permanent unsteadiness alternating with episodes of vertigo. ENG (VOR) showed a severe hyporeflexia of the right labyrinth (41%) and the horizontal semicircular function out of balance (35% directional preponderance to the right). She presented a PTA of 36 dB HL (right) and 40 dB HL (left), with nearly symmetrical steep downward curves starting from 1,500 Hz (Figs. 9, 10 and 11). No lesions could be demonstrated on CT or MR imaging.

Patient 8 (family III) presented at the age of 46 years with a history of hearing impairment and subtle imbalance for more than 20 years (34 years of age, see Table 2). Five years earlier, he had undergone a tympanoplasty at the right ear. At the first visit, his hearing levels were 68 dB HL PTA (right) and 8 dB HL PTA with high frequency loss (left) (Figs. 9, 10 and 11). He also experienced from multiple telangiectasia with nose bleedings because of

a hereditary hemorrhagic telangiectasia (HHT, Osler-Weber-Rendu disease). CT imaging did not show any abnormality, except for a remodelled ossicular chain at the right side.

At the age of 51 years, he returned to our department because of rapid otovestibular deterioration resembling Ménière-like syndrome, with hearing levels of 90 dB HL PTA (right) and 58 dB HL PTA (left) (Figs. 9, 10 and 11). Vestibular examination (VOR) using ENG revealed a total areflexia of the right vestibular organ with complete central compensation (normal rotational chair tests). New CT and MRI imaging showed signal loss in the PSCC on the right and possibly faintly in the LSCC as compared with the healthy patient's left side (Fig. 7B). These findings corresponded with a discrete hyperdensity in the PSCC on the right on CBCT (Fig. 7A).

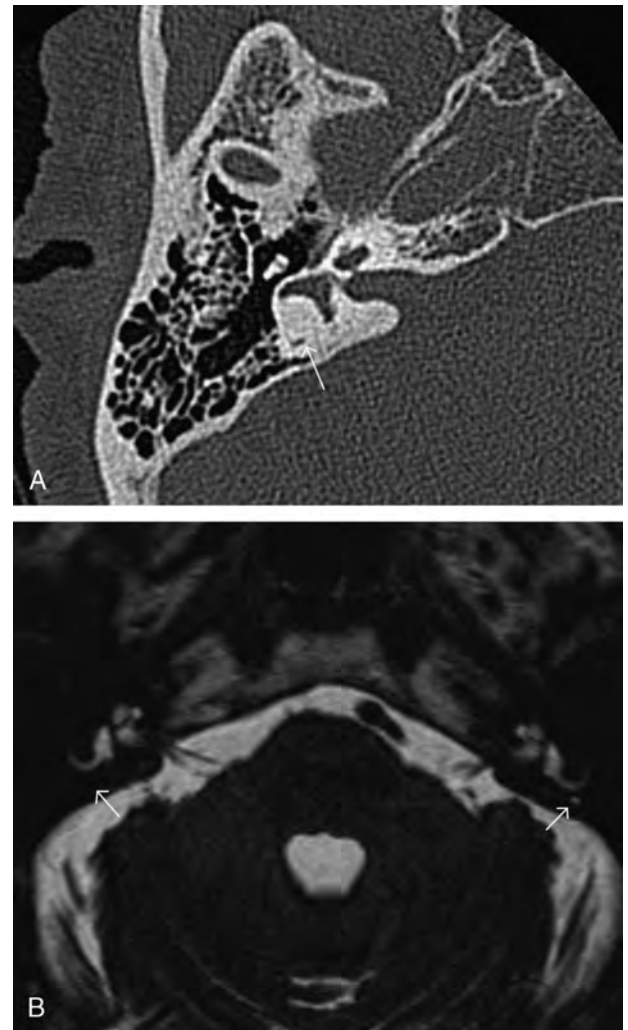


FIG. 6. A and B, CT and MR imaging of Patient 6: (A) Patient 6: axial CT of the right temporal bone showing focal subtle narrowing of the PSCC. B, patient 6: axial MR (Achieva) image: absent fluid signal in the PSCC on the patient's right side, compared with the normal signal on the left (arrows).

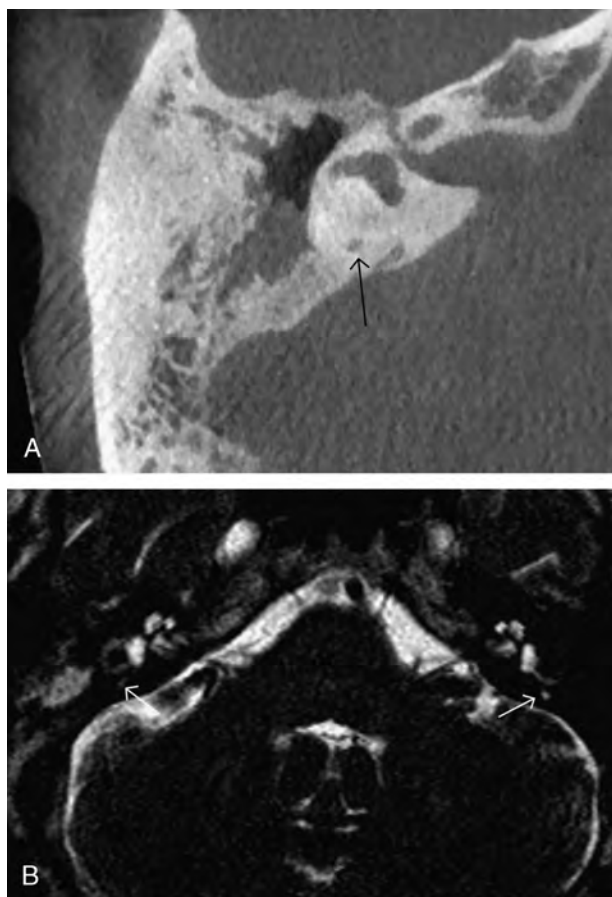


FIG. 7. A and B, CT and MR imaging of Patient 8: (A) Patient 8: axial CBCT image showing subtle higher density in the PSCC (arrow) (compare with the normal signal in the vestibulum). B, Patient 8: axial MR (NT Scan) images: decreased intensity of the fluid signal in the PSCC on the patient's right side (compared with the normal signal on the contralateral side (arrows)). Partial volume effect in the right LSCC.

Finally, patient 9, mother of patient 8(III), showed hearing levels of 100 dB HL PTA (right) and 95 dB HL PTA (left) (Figs. 9, 10 and 11). Like her son, she also had facial and oral telangiectasia due to Osler-Weber-Rendu disease (HHT).

CT scan showed a clear focal area of sclerosis in the left LSCC (Fig. 8A and B). MR imaging revealed signal loss in the posterior half of the vestibule on the right side and also signal loss at the most lateral portion of the left LSCC (Fig. 8C).

In summary, similar focal sclerotic lesions and/or narrowings in one or more semicircular canals were demonstrated on CT scan in eight of 9 patients, with a corresponding signal loss on T2-weighted MR imaging. In 1 patient, signal loss was also described in the posterior part of the vestibulum.

In 58% of the cases, the posterior semicircular canal (PSCC) was affected, whereas the superior (SSCC), lateral (LSCC) and vestibule were affected in 21%, 16% and 5%, respectively. Thirty-one percent (31.6%) of the lesions

on MR imaging were not detected on CT scans, suggesting fibrosis at these sites. The median threshold of the hearing loss in ears presenting these lesions was 104 dB HL PTA (ranging from 78 to 120 dB HL) compared with 58 dB HL PTA for those ears without any radiologic abnormality (range: 8–76 dB HL), which is statistically significant (Mann-Whitney U test, $p < 0.001$) for all frequencies, except for 6 kHz ($p < 0.05$) (Figs. 9 and 10A and B).

DISCUSSION

DFNA9 is an autosomal dominantly inherited form of hearing impairment which is characterized by late onset otovestibular deterioration. It has been linked to a variety of mutations in the COCH gene and one of them, the P51S mutation, is known to be very common in the Low Countries (Belgium and The Netherlands) because of a common founder (2–7,12–15).

During the last decade, many phenotype-genotype correlative reports helped to characterize the phenotype of this hereditary disease, including both its audiological and vestibular aspects, showing very little variability across subjects (2–9).

Here we report radiographic abnormalities involving the semicircular canals in eight out of a series of nine mutation carriers (Table 1). To our knowledge, we are the first to report these findings.

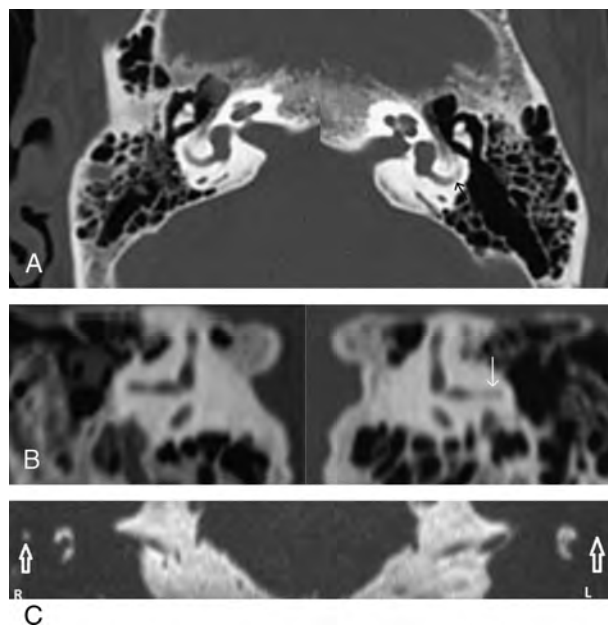


FIG. 8. A, B, and C, CT and MR imaging of Patient 9: (A) Patient 9: Lightspeed 16-slice scanner (GE, Milwaukee, USA). Axial CT images of both temporal bones: arrow on an area of focal sclerosis in the left LSCC. B, patient 9: coronal CT image reconstructions confirming the sclerosis (arrow) on the left. C, Patient 9: 1.5 T Avanto (Siemens, Erlangen, Germany) 3D TSE T2-weighted images clear signal loss at the most lateral portion of the left LSCC (arrows).

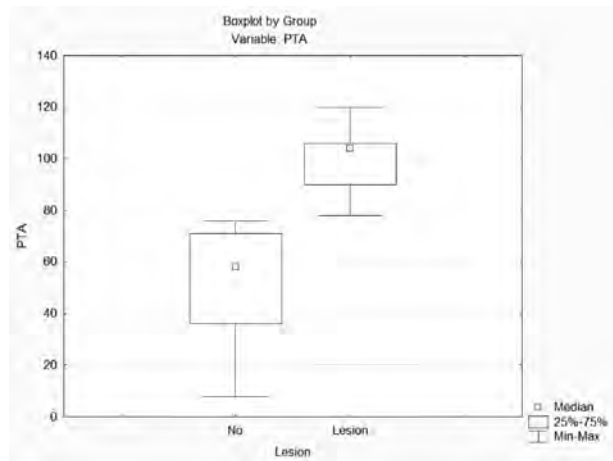


FIG. 9. Hearing thresholds (PTA in dB HL) with and without CT/MRI lesions. PTA displayed in y-axis represents the pure tone average measured at 500, 1,000, 2,000, and 3000 Hz and expressed in dB HL. The “no” group represents those ears showing no lesions on radiologic data; the “lesion”-group represents the ears with anomalies detected on CT/MR imaging (Table 1). Mann-Whitney U test: $p < 0.000026$ ($p < 0.001$).

Of the patients who demonstrated loss of signal in the semicircular canals on MR imaging, only 68,4% had corresponding CT findings. This suggests that fibrosis may be the initial pathology, followed by ossification. This observation was seen in patients numbered 2,3,5,6,8, and 9 (see previous section, Tables 1 and 2). Patient 2, more specifically, had a signal loss at the PSSC as well as the SSCC while the CT scans detected only abnormalities at the SSCC. MR images of patient 3 showed signal loss in both the right and left PSSC, whereas on CT scan, only the right PSSC featured abnormalities. The fifth patient had a complete and bilateral signal loss of the PSSC on MRI, whereas on CT scan, the left side only showed a partial sclerosis. In Patient 6, MRI lesions were detected at the SSCC and PSSC of the right ear, whereas only the PSSC was affected on CT scan. Also, Patient 8 displayed a complete signal loss at the PSSC and a faint loss at the LSCC on MRI with only a discrete PSSC hyperdensity on CT scan. Finally, in Patient 9, both MRI and CT imaging demonstrated focal sclerosis of the left LSCC, whereas only MR imaging was also able to detect a signal loss of the posterior part of the right vestibule.

Seven of the 9 patients we studied belong to 3 anamnestically unrelated families: family I (Patients 3, 4, and 5), family II (Patients 6 and 7), and family III (Patients 8 and 9). The degree of hearing impairment of Patients 2, 3, 4, 5, 6, and 9 was already advanced by the time of the investigation, whereas Patients 7 and 8 were seen at more early stages. It is noteworthy that (focal) sclerosis on radiologic investigation was obvious in all patients with pronounced hearing loss (see below).

All members of family I (Patients 3, 4, and 5) showed clearly visible and similar sclerotic lesions and were all in advanced disease stage with very poor hearing function. The members of the other 2 families (II and III) were each

examined at different stages, making it difficult to draw conclusions. Patient 7 (family II) was probably investigated in an early stage with a bilateral high frequency hearing loss. Her elder brother (Patient 6) had more advanced hearing loss and did show lesions on medical imaging. Patient 8 (family III) was documented twice with a 5-year interval. First, the radiologic investigation was unremarkable (except for the ossicular reconstruction, see previous section), but 5 years later, lesions were visible, indicating a more advanced stage (Table 1). His mother, Patient 9, presented in a very advanced stage of the disease, and she also presented the radiologic findings.

The interpretation of the abnormalities in Patient 6 (family II) though is less straightforward because he had experienced a postintervention hearing loss. The CT and MRI findings may therefore be biased. However, the site and type of lesion is comparable to the other patients of this series and are unlikely to be caused by a surgical intervention.

The strong correlation between the severity of the hearing impairment and the presence of lesions on CT and MRI

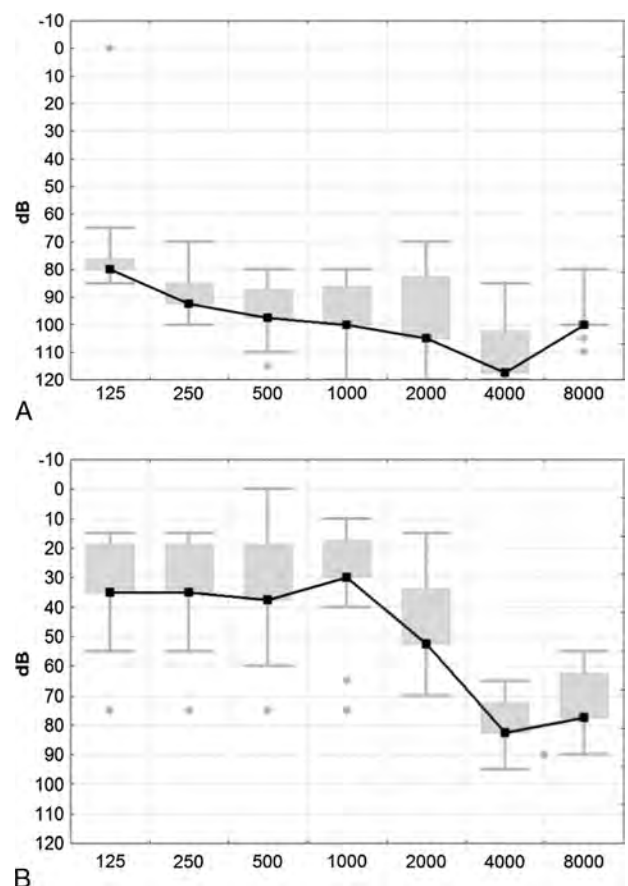


FIG. 10. A and B, Box and whisker plots of the hearing thresholds displayed per frequency (PTA in dB HL) of all patients. Fig “A” represents the ears presenting radiologic abnormalities, and Fig “B” gives an overview of the thresholds of the unaffected ears. The Mann-Whitney U test were significant ($p < 0.001$) for all frequencies, except for 6 kHz ($p < 0.05$).

is remarkable (Figs. 9, 10 and 11; Table 1), with a median loss of 104 dB HL in case of lesions compared with 58 dB HL in absence of radiologic findings. This strong difference ($p < 0,001$) suggests an interdependency between the radiologic findings and the degree of hearing loss, and it seems reasonable to assume that both are linked to the stage of the disease.

Unfortunately, this series does not allow correlating the radiologic findings with the degree of vestibular deterioration because the vestibulo-ocular reflex (VOR) tests (ENG) were only performed in 3 subjects (Table 2). Although all subjects reported vestibular symptoms having existed for many years by the time of their first visit, these were rarely the main complaint. Most subjects didn't even mention them spontaneously. When explicitly asked, most subjects articulated their vestibular symptoms as unsteadiness in the dark and increasing sense of instability and dizziness. Unsteadiness and instability in the dark was observed in all subjects aged 60 years or older (Table 2).

Bischoff et al. demonstrated in a large DFNA9 family study that vestibular impairment starts earlier (around the age of 34 yr), progresses more rapidly, and is usually more complete than the hearing impairment in P51S mutation carriers, with severe hyporeflexia observed around the age of 40 years, and total areflexia completed in the fifth decade (2,9). The vestibular signs described in Table 2 are also in line with these expectations.

The VOR test of Patient 7 (II) showed severe hyporeflexia at the age of 49, which is also in accordance with Bischoff's description. It is noteworthy that in this patient no radiologic abnormalities were detected.

Hildebrand et al. reported a DFNA9 case with bilateral superior SCC dehiscence identified at the age of 31 years (11). The CT scan did not show focal sclerosis. This may be explained by the patient's relatively young age, and our current finding that such lesions may only become apparent at later stages. It should be noted that the subjects described by Hildebrand were carrying a different COCH mutation (G88E) as compared with patients in this series

(11). As all our patients carry the same P51S mutation, it remains currently unclear whether the radiologic characteristics we discovered are also present in patients with other COCH mutations. However, our findings indicate that focal sclerosis is a common finding in advanced DFNA9 caused by the P51S mutation, and it seems reasonable to speculate that it could also be the case for other COCH mutations.

The subjects in this report were documented by both CT and MR imaging and most featured an advanced degree of otovestibular impairment. This is in contrast with other reports where the subjects were younger and less documented by medical imaging (2–11). Therefore, it is well possible that these radiologic findings were not yet present in most patients and, hence, have escaped detection (2,9,11). Radiologic investigation of patients with other COCH mutations in an advanced disease stage will be an easy and rapid way of resolving this issue.

It remains unclear what really causes the sclerosis of the SCC. Because no enhancement of the SCC was seen after admission of gadolinium on T1-weighted images, the radiologic findings could be an end-phase of a slowly progressing inflammatory reaction, comparable with post-meningitic labyrinthine fibrosis followed by ossification, albeit slower and less aggressive in case of DFNA9. An alternative hypothesis could relate to protein misfolding and eosinophilic cochlin-containing deposits (17,18).

Because of the late appearance of such radiologic findings in DFNA9 patients, radiologic investigation probably does not offer benefits for an early DFNA9 diagnosis in patients suffering of progressive otovestibular deterioration. We remain convinced that molecular genetic analysis still remains the most important investigation to identify DFNA9. We consider the combination of CT and MRI good clinical practice in certain cases to differentiate between DFNA9 and other diseases such as Ménière's disease, cerebellopontine angle tumors, multiple sclerosis, dehiscent superior semicircular canal syndrome, and so on. Medical imaging may be particularly indicated whenever cochlear and/or vestibular implantation is considered or in case of more complex Ménière-like history (20,21).

A final consideration goes to the possibility that the radiologic findings in DFNA9 patients are resulting from modifier genes (22–24). During the last decade, our understanding of hereditary hearing loss has been refined by functional studies of modifier genes of a number of hearing loss loci (22,23). The study of genetic modifiers for monogenic diseases presents opportunities for diseases with reduced penetrance, variable expressivity or a high phenotypic variability (22–24). These types of variability can be due to other genetic factors, that is, genetic modifiers. However, for DFNA9 the phenotype is exceptionally uniform and the penetrance is complete (2–11). Before genetic modifiers for DFNA9 could play a role of any importance, we would need to see much more clinical heterogeneity between patients with the same mutation. Hundreds of patients with the P51S mutation have been reported in the literature, and the group is phenotypically very homogeneous (2–11), as it is also the case in this case series. It

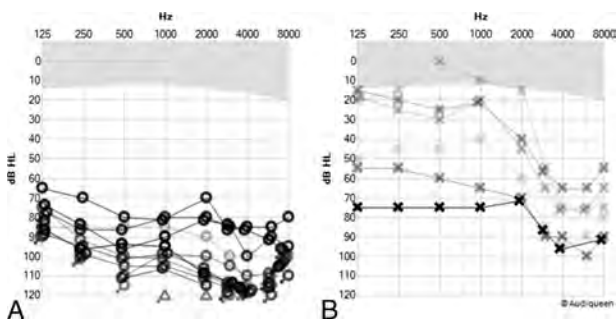


FIG. 11. Overview of all hearing thresholds of Patients 1–9. The thresholds of Patient 8 at first and second visits are also represented because the radiologic lesions appeared on the second radiologic investigation. Column A : all hearing thresholds of the ears with radiologic lesions (range, 78–120 dB HL PTA; median, 104 dB HL PTA), B: All hearing thresholds of the unaffected ears (range: 8-76 dB HL PTA, median: 58 dB HL PTA).

is therefore unlikely that the radiologic findings are the result of any modifier gene in DFNA9.

CONCLUSION

In this paper, the authors report radiologic findings in 8 patients with the P51S missense mutation causing DFNA9 otovestibular dysfunction, consisting of similar sclerotic lesions and corresponding signal losses on CT and MR imaging at the level of one or more semicircular canals. These radiologic abnormalities seem to coincide with more advanced degrees of the otovestibular deterioration. We conclude that a new phenotypic and characteristic radiologic feature of COCH P51S mutation carriers has been discovered. It seems likely that these findings are not exclusively encountered in P51S COCH mutation carriers but may also occur in other COCH mutations. It would be interesting to compare these findings to a larger series of COCH mutation carriers, including mutations different from P51S.

Acknowledgments: The authors thank Bert De Foer, M.D., Ph.D., Department of Radiology, Sint-Augustinus Hospital, Antwerp-Wilrijk, Belgium, for providing the medical imaging of Patient 9.

They also thank Mary Elisabeth Cunnane, M.D., Department of Radiology, Massachusetts Eye and Ear, Boston, USA, for revising the English language throughout the manuscript.

REFERENCES

- Hildebrand MS, Gandolfo L, Shearer AE, et al. A novel mutation in COCH-implications for genotype-phenotype correlations in DFNA9 hearing loss. *Laryngoscope* 2010;120:2489–93.
- Kemperman MH, De Leenheer EMR, Huygen PLM, et al. Audiometric, vestibular, and genetic aspects of a DFNA9 family with a G88E COCH mutation. *Otol Neurotol* 2005;26:926–33.
- Fransen E, Verstreken M, Bom SJH, et al. *J Med Genet* 2001; 38:61–5.
- Verhagen WIM, Bom SJH, Fransen E, et al. Hereditary cochleovestibular dysfunction due to a COCH gene mutation (DFNA9): a follow-up study of a family. *Clin Otolaryngol* 2001;26:477–83.
- Lemaire FX, Feenstra L, Huygen PLM, et al. Progressive late-onset sensorineural hearing loss and vestibular impairment with vertigo (DFNA9/COCH): longitudinal analysis in a Belgian family. *Otol Neurotol* 2003;24:743–8.
- Pauw RJ, Huygen PLM, Collin RWJ, et al. Phenotype description of a novel DFNA9/COCH mutation, I109T. *Ann Otol Rhinol Laryngol* 2007;116:349–57.
- Verstreken M, Declau F, Wuyts FL, et al. Hereditary otovestibular dysfunction and Ménière's disease in a large Belgian family is caused by a missense mutation in the COCH gene. *Otol Neurotol* 2001; 22:874–81.
- BOM SJH, Kemperman MH, Huygen PLM, Lijndijk MWJ, Cremers CWRJ. Cross-sectional analysis of hearing threshold in relation to age in a large family with cochleovestibular impairment thoroughly genotyped for DFNA9/COCH. *Ann Otol Rhinol Laryngol* 2003;112:280–6.
- Bischoff AMLC, Huygen PLM, Kemperman MH, et al. Vestibular deterioration precedes hearing deterioration in the P51S COCH mutation (DFNA9): an analysis in 74 mutation carriers. *Otol Neurotol* 2005;26:918–25.
- De Kok YJM, BOM SJH, Brunt TM, et al. A Pro 51Ser mutation in the COCH gene is associated with late onset autosomal dominant progressive sensorineural hearing loss with vestibular defects. *Hum Mol Genet* 1999;8:361–6.
- Hildebrand MS, Tack D, DeLuca A, et al. Mutation in the COCH gene is associated with superior semicircular canal dehiscence. *Am J Med Genet Part A* 2009;149A:280–5.
- Robertson NG, Resendes BL, Lin JS, et al. Inner ear localization of mRNA and protein products of COCH, mutated in the sensorineural deafness and vestibular disorder, DFNA9. *Hum Mol Genet* 2001;10:2493–500.
- Robertson NG, Cremers CWRJ, Huygen PLM, et al. Cochlin immunostaining of inner ear pathologic deposits and proteomic analysis in DFNA9 deafness and vestibular dysfunction. *Hum Mol Genet* 2006;15:1071–85.
- Robertson NG, Jones SM, Sivakumaran TA, et al. A targeted COCH missense mutation: a knock-in mouse model for DFNA9 late-onset hearing loss and vestibular dysfunction. *Hum Mol Genet* 2008; 17:3426–34.
- Robertson NG, Hamaker SA, Patriub V, Aster JC, Morton CC. Subcellular localisation, secretion, and post-translational processing of normal cochlin, and of mutants causing the sensorineural deafness and vestibular disorder, DFNA9. *J Med Genet* 2003;40:479–86.
- Street VA, Kallman JC, Robertson NG, Kuo SF, Morton CC, Phillips JO. A novel DFNA9 mutation in the vWFA2 domain of COCH alters a conserved cysteine residue and intrachain disulfide bond formation resulting in progressive hearing loss and site-specific vestibular and central oculomotor dysfunction. *Am J Med Genet A* 2005;139:86–95.
- Khetarpal U. DFNA9 is a progressive audiovestibular dysfunction with a microfibrillar deposit in the inner ear. *Laryngoscope* 2000; 110:1379–84.
- Merchant SN, Linthicum FH, Nadol JB Jr. Histopathology of the inner ear in DFNA9. *Adv Otorhinolaryngol* 2000;56:212–7.
- Committee on Hearing and Equilibrium guidelines for the evaluation of results of treatment of conductive hearing loss. American Academy of Otolaryngology–Head and Neck Surgery Foundation, Inc. *Otolaryngol Head Neck Surg* 1995;113:186–7.
- Van de Berg R, Guinand N, Stokroos RJ, Guyot J-P, Kingma H. The vestibular implant: quo vadis? *Front Neurol Neurotol* 2011;113:1–7.
- Van de Berg R, Guinand N, Guyot J-P, Kingma H, Stokroos RJ. The modified ampullar approach for the vestibular implant surgery: feasibility and its first application in a human with a long-term vestibular loss. *Front Neurol Neurotol* 2012;1–8.
- Friedman Th, Battey J, Kacher B, et al. Modifier genes of hereditary hearing loss. *Curr Opin Neurobiol* 2000;10:487–93.
- Riazuddin S, Ahmed Z, Friedman Th, Griffith A, Riazuddin S, Wilcox E. Genetic modifiers of hereditary hearing loss. In: Genetic hearing impairment. In: Cremers Cor WRJ, Smith RJH, eds. *Adv Otorhinolaryngol*. Basel: Karger, 2002;61:224–9.
- Kallman JC, Phillips JO, Bramhall NF, Kelly JP, Street VA. In search of the DFNA11 myosin VIIA (MYO7A) low and mid-frequency auditory genetic modifier. *Otol Neurotol* 2008; 29:860–7.